Applied Materials Today 16 (2019) 375–387

Contents lists available at ScienceDirect

Applied Materials Today

journal homepage: www.elsevier.com/locate/apmt

Lithium-calcium-silicate bioceramics stimulating cementogenic/osteogenic differentiation of periodontal ligament cells and periodontal regeneration

Qian Zhang[a,1], Lei Chen[b,1], Bin Chen[a], Changxing Chen[a], Jiang Chang[b], Yin Xiao[c], Chengtie Wu[b,*], Fuhua Yan[a,*]

[a] Nanjing Stomatological Hospital, Medical School of Nanjing University, 30 Zhongyang Road, Nanjing, Jiangsu 210008, PR China
[b] State Key Laboratory of High Performance Ceramics and Superfine Microstructure, Shanghai Institute of Ceramics, Chinese Academy of Sciences, 1295 Dingxi Road, Shanghai 200050, PR China
[c] The Institute of Health and Biomedical Innovation, Queensland University of Technology, 80 Musk Avenue, Queensland 4059, Australia

ARTICLE INFO

Article history:
Received 29 May 2019
Received in revised form 21 June 2019
Accepted 21 June 2019

Keywords:
Lithium-calcium-silicate bioceramics
Periodontal ligament cells
Signaling pathway
Periodontal regeneration

ABSTRACT

The ultimate goal of treatment of periodontal disease is not only to control inflammation and further to prevent development of the lesion, but also to achieve regeneration of the destroyed periodontal tissue. This study aimed to investigate the effect of lithium-calcium-silicate ($Li_2Ca_4Si_4O_{13}$, LCS) bioceramics on the cementogenic/osteogenic differentiation of human periodontal ligament cells (PDLCs) and regeneration of periodontal tissue as well as the corresponding mechanism. We prepared LCS bioceramics and explored the cementogenic/osteogenic differentiation of PDLCs after cultured with LCS extracts *in vitro*. Meanwhile, we further studied the involvement of the Wnt/β-catenin and ERK signaling pathway during this process. In the *in vivo* study, the regeneration of alveolar bone defect in New Zealand white rabbits and the periodontal tissue in beagle dogs were compared by applying LCS and β-tricalcium phosphate (β-TCP). Our results showed that a certain concentration of LCS extracts could significantly stimulate cementogenic/osteogenic differentiation of PDLCs, including alkaline phosphatase (ALP) activity, periodontal regeneration-related gene expression, Wnt/β-catenin and ERK signaling pathway related gene expression and protein expression of PDLCs. Moreover, it was found that LCS bioceramics could significantly activate Wnt/β-catenin and ERK signaling pathway in cementogenesis/osteogenesis of PDLCs. The *in vivo* results suggested that LCS significantly promoted the regeneration of bone defects and periodontal defects as compared with β-TCP in rabbit and beagle dog models, in which the LCS bioceramics possess the capacity to trigger the activation of the two signaling pathway, leading to significantly improved periodontal regeneration. Our study suggests that LCS is a promising bioactive material for periodontal regeneration, consequently offering a promising treatment strategy for the treatment of periodontitis-related disease.

1. Introduction

Periodontal disease is not only the leading cause of tooth loss in adults, but a large number of studies have also confirmed that periodontal disease is closely related to some systemic diseases [1,2]. It has always been a challenging issue in the treatment of periodontal disease for how to effectively treat periodontitis and achieve periodontal regeneration, and a research hotspot of researchers for a long time. Ideal strategies should be able to repair and regenerate all damaged structures including the periodontal ligament, cementum, and alveolar bone.

At present, there are various materials available for periodontal and alveolar bone regeneration, which can be divided into natural graft tissues (autografts, allografts and xenografts) and synthetic materials (alloplasts) [3–5]. Autogenous bone grafts have generally good biocompatibility and regeneration efficiency; however, extra wound, donor site morbidity and limited graft volume are their main disadvantages. Allografts are available in large amounts for use, while the possibility of tissue contamination, persistent antibody-negative carriers and disease transmission with new unidentified pathogens limit their application [5]. The xenografts, most commonly used in periodontal regeneration are the deproteinized bovine bone mineral, commercially known as Bio-Oss®, which is a commercially available bone of bovine origin [6].

* Corresponding authors.
E-mail addresses: chengtiewu@mail.sic.ac.cn (C. Wu), yanfh@nju.edu.cn (F. Yan).
[1] Co-first authors.

https://doi.org/10.1016/j.apmt.2019.06.011

Bio-Oss® has high osteoconductive potential; however, these grafts are inherently fragile and lack toughness, which makes them prone to failure [7–9]. The most routinely used clinically alloplastic materials for periodontal bone regenerations over the last few years were hydroxyapatite (HA), β-tricalcium phosphates (β-TCP), bioactive glasses [5]. They have generally good biocompatibility; however, their degradation and regeneration efficiency are not optimal [5]. In recent years, as a new type of biomaterial, silicate bioceramics have been studied for bone tissue engineering [10,11]. Silicate bioceramics have been shown to be bioactive and resorbable and they are suitable for bone tissue engineering applications due to their excellent bone-forming activity [12]. It was found that silicon (Si) ions could stimulate the osteogenic differentiation of human bone marrow stromal cells (hBMSCs) via activating their ALP activity, bone-related gene and protein expression [13]. Our previous studies demonstrated that silicate-based bioceramics possessed excellent mineralization bioactivity and their ionic products are able to enhance cell proliferation, osteogenic differentiation and new bone formation as well as angiogenesis and osteochondral defect regeneration [14–18].

Lithium (Li) is widely used as a long-term mood stabilizer for the treatment of depression. Previous studies had shown that LiCl salt can stimulate chondrocyte proliferation, selectively inhibits phosphorylation and protects cartilage from degradation [19–21]. It was reported that the LiCl could stimulate subchondral bone formation and enhance bone mass [22–24]. Our previous study found that Li-containing porous scaffolds could promote the regeneration of both cartilage and subchondral bone *in vivo* [25]. In addition, Li could be used for inducing proangiogenesis and vascularization by eliciting the expression of exosomes [26,27]. Although the use of Li salt and Li-containing biomaterials as a reagent for bone/cartilage regeneration have been reported, there is few studies about Li-containing biomaterials for regeneration of periodontal tissues, especially in the *in vivo* study for large animal models and the corresponding mechanism is still unclear.

Therefore, based on the positive effect of Si and Li ions on bone tissues, we hypothesized that if we synthesize new biomaterials containing Si and Li and other elements, which may be used for the regeneration of periodontal defects by harnessing their ionic bioactivities. We have recently synthesized lithium-calcium-silicate (LCS) bioceramics. Due to its specific composition and structure, we speculated that LCS has ions-synergetic effects on the regeneration of periodontal tissue. In this study, the effects of ionic products from LCS on the cementogenic/osteogenic and angiogenic differentiation of periodontal ligament cells (PDLCs) and the corresponding mechanism were systematically investigated. Meanwhile, the regeneration capacity of LCS in periodontal tissue both in rabbit and beagle dog models was investigated by comparing with conventional β-TCP bioceramics (see Scheme 1). It is expected that the study will pave the way for periodontal regeneration by using high activity of biomaterials.

2. Materials and methods

2.1. Synthesis of LCS powders and preparation of LCS granules

Lithium-calcium-silicate bioceramic powders ($Li_2Ca_4Si_4O_{13}$, LCS) were synthesized by sol-gel process using tetraethyl orthosilicate ($(C_2H_5O)_4Si$, TEOS), calcium nitrate tetrahydrate ($Ca(NO_3)_2{\cdot}4H_2O$) and lithium nitrate ($LiNO_3$) (all from Sinopharm Chemical Reagent Co., Ltd., Shanghai, China) according to our previous study [25]. The content of Li elements in the compound is around 4.1% (wt.%).

For preparation of LCS granules used for the *in vivo* study, the obtained LCS powders were mechanically mixed with 6 wt.% polyvinyl alcohol binders with the ratio of 0.01 (binders/LCS powder mass), then the mixtures were uniaxially pressed at 16 MPa in a cylindrical mold (Ø40 mm) to obtain the LCS green compacts. The LCS ceramics were fabricated by sintering the LCS green compacts at 950 °C for 3 h with a heating rate of 2 °C/min to remove the binders. Subsequently, the LCS ceramics were crushed into small particles and sieved. The granules between 20 and 40 mesh were used as following animal experiments. The size of the prepared granules was in the range of 420–840 μm. As the control materials, β-TCP granules were prepared by the same method as described above and sintered at 1100 °C for 3 h.

2.2. Preparation of the dissolution extracts of LCS powders

The LCS powders were weighed and the dissolution extracts of LCS were prepared by soaking LCS powders to low glucose Dulbecco's Modified Eagle Medium (DMEM-LG, Gibco, Grand Island, NY, USA) at the concentration of 200 mg/mL according to International Standard Organization (ISO/EN) 10993-5 [28]. After incubated at 37 °C for 24 h, the mixture was centrifuged and the supernatant was collected. Then, gradient dilutions of extracts (100 mg/mL, 75 mg/mL, 50 mg/mL, 25 mg/mL, 12.5 mg/mL, 6.25 mg/mL) were prepared with serum-free DMEM-LG. The extracts were sterilized by using a 0.2 μm filter and supplemented with 10% fetal calf serum (FCS, Gibco, Life Technologies, USA) and 1% penicillin/streptomycin (P/S, HyClone, South Logan, UT, USA) for further cell experiments. The DMEM-LG supplemented with 10% FCS and 1% P/S without addition of LCS extracts was used as a blank control (0 mg/mL).

2.3. Cell culture

Human periodontal ligament cells (hPDLCs) were purchased from ScienCells, LLC (Carlsbad, CA, USA). The cells were then passaged and proliferated. The third generation of hPDLCs with good growth status was used in this experiment.

2.4. The effect of LCS extracts on the proliferation and alkaline phosphatase (ALP) activity of hPDLCs

The proliferation of hPDLCs in the LCS extracts was examined with CCK-8 assay. Briefly, hPDLCs were seeded in 96-well plates at an initial density of 2×10^3 cells in 200 μL of medium per well. Then, the medium were changed into different concentration of the LCS extracts (0, 6.25, 12.5, 25, 50, 75, 100 and 200 mg/mL) in DMEM-LG supplemented with 10% FCS and 1% P/S. On day 2, 4 6 and 8, 20 μL of CCK-8 solution (Tongren medicine, Japan) was added to each well and incubated at 37 °C, 5% CO_2 for 3 h. A microplate reader was then used to read the absorbance values in different wells at a wavelength of 450 nm to compare cell activities between different groups at room temperature. All the results were expressed as the optical density (OD) value minus the absorbance of blank wells and experiments were repeated in triplicate.

Third generation of hPDLCs were inoculated into 6-well plates at a density of 5×10^4 cells/well. Different concentrations of LCS medium were added according to different groups and cultured at 37 °C, 5% CO_2, and the medium were changed every other day. The relative ALP activity of hPDLCs was assessed on day 7 and 14 by using the ALP Assay kit (Sigma–Aldrich, St. Louis, MO, USA). At each time point, the cells were digested with 0.25% trypsin-EDTA (Gibco, Grand Island, NY, USA) and counted, then 1×10^5 cells of each group were washed with PBS three times to remove the residual medium, and then resuspend cells in 80 μL of Assay Buffer. Centrifuge samples at 4 °C at top speed in a cold microcentrifuge to remove any insoluble material. The supernatant was collected as the samples to be tested. Preparation of ALP standards with

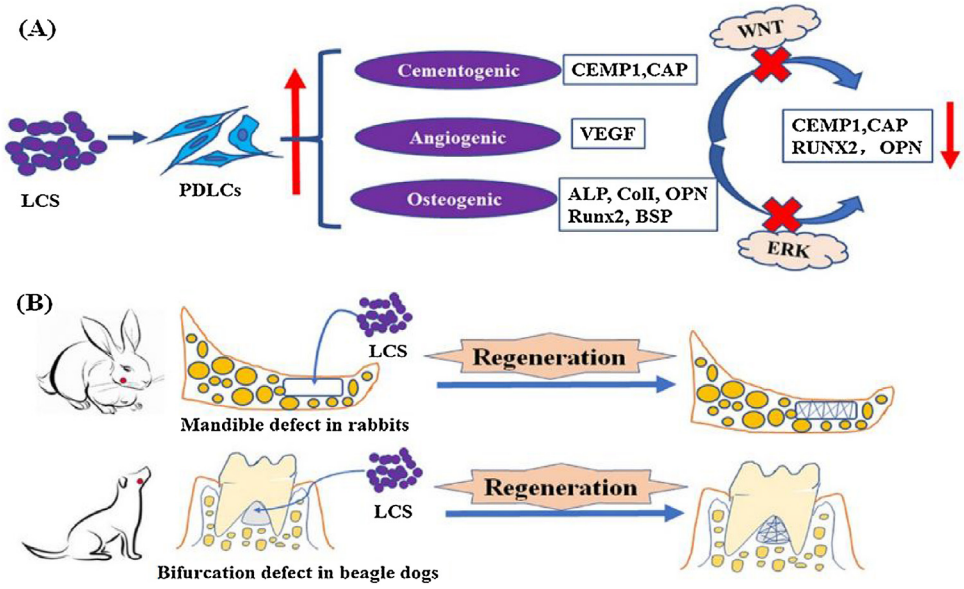

Scheme 1. Schematic illustration of application of LCS for periodontal reconstruction. The LCS powders could significantly stimulate cementogenic/osteogenic differentiation of periodontal ligament cells *in vitro* (A); on the other hand, LCS granules significantly accelerated alveolar bone regeneration as well as promoted vascularization of alveolar bone *in vivo* (B).

Table 1
The primer sequence used in the real-time PCR analysis.

Primer	Forward sequences	Reverse sequences
GAPDH	TCAGCAATGCCTCCTGCAC	TCTGGGTGGCAGTGATGGC
ALP	CACGCCCTTTGCTTTATCT	TCTGAGCCTCCTCTTTTCCT
Runx2	CAGACAGAAGCTTGATGACTCTAA	CGGGACACCTACTCTCATACT
OPN	TCACCTGTGCCATACCAGTTAA	TGAGATGGGTCAGGGTTTAGC
Wnt3a	TGGACAAAGCTACCAGGGAGT	CCCACCAAACTCGATGTCCTC
OCN	GCAAAGGTGCAGCCTTTGTG	GGAAAGAAGGGTGCCTGGAGAG
β-Catenin	CTTCACCTGACAGATCCAAGTC	CCTTCCATCCCTTCCTGTTTAG
BSP	CTGGCACAGGGTATACAGGGTTAG	ACTGGTGCCGTTTATGCCTTG
MMP2	AAGTGGTCCGTGTGAAGTATG	GGTATCAGTGCAGCTGTTGTA
CAP	CTGCGCGCTGCACATGG	GCGATGTCGTAGAAGGTGAGCC
CEMP1	GGGCACATCAAGCACTGACAG	CCCTTAGGAAGTGGCTGTCCAG
FN	GTATCCCTCGTGGCCATAAA	TCGGTGTTGTAAGGTGGAATAG
VEGF	CATGCAGATTATGCGGATCAA	GCATTCACATTTGTTGTGCTGTAG
Col I	CTTTGGAGCCAGCTGGA	GTGGGCTTCCTGGTGA

different concentration gradients according to the manufacturer's protocol. 50 μL of 5 mM pNPP solution were added and the mixtures were incubate at 25 °C for 60 min protected from light. The sample wells and standard reactions were stopped by adding 20 μL Stop Solution. The optical density (OD) was measured at 405 nm with a spectrophotometer. A standard curve was drawn to calculate the amount of ALP in each well. From this result, a histogram of the ALP concentration of each group of cells was analyzed and plotted on GraphPad Prism.

2.5. The effect of LCS extracts on osteogenic/cementogenic differentiation and angiogenic gene/protein expression of hPDLCs

Total RNA was extracted from hPDLCs cultured in different concentrations of the LCS extract on day 7 and day 14 with Trizol reagent (Invitrogen, USA). Then complementary DNA was synthesized using the SuperScript® VILO™ cDNA synthesis kit (Thermo Fisher Scientific, Waltham, MA, USA) for reverse transcription. The RT-qPCR primers (Table 1) were designed based on cDNA sequences from the NCBI. TaqMan gene expression assay kits (Applied Biosystems, Grand Island, NY) were used to perform real-time quantitative PCR following the manufacturer's instructions. All reactions were run in triplicate for three independent experiments. The mRNA expression levels in different groups were quantitatively compared by using the $\Delta\Delta T$ method and expressed as $2^{-\Delta\Delta T}$.

RIPA lysate (Beyotime, China) was used to lyse cells in different concentrations of the LCS extract on day 7 and to extract total protein for Western blot. ALP (rabbit anti-human; Abcam, USA), OPN (rabbit anti-human; Abcam, USA), Runx2 (rabbit anti-human; Abcam, USA), CEMP1 (rabbit anti-human; Abcam, USA), Wnt3a (mouse anti-human; Abcam, USA), Col I (mouse anti-human; Abcam, USA), p-ERK (rabbit anti-human; Abcam, USA), ERK (mouse anti-human; Abcam, USA) were served as primary antibody and β-actin expression served as an internal reference. Band intensities were quantified by scanning densitometry and gray level analysis was performed using the ImageJ software. The above experiments were repeated 3 times under the same condition.

Third generation of hPDLCs were seeded in a 6-well plate at a density of 3×10^5 cells/well, then cultured in the presence of different concentration of LCS extracts. On days 7 and 14 during cultivation, the supernatants were collected from cells in different groups. A Quantikine Elisa kit (R&D Systems, Minneapolis, MN, USA) was used to detect the concentrations of VEGF in the collected supernatants. Three identical wells were used for each group at two time points.

2.6. The effects of Wnt/β-catenin and ERK signaling pathways on osteogenic/cementogenic differentiation of hPDLCs cultured in LCS extracts

Third generation of hPDLCs were seeded in a 6-well plate at a density of 3×10^5 cells/well, three concentration of LCS (0, 25, 50 mg/mL) were selected. The effect of the Wnt/β-catenin signaling pathway on hPDLCs cultured in LCS extracts was further investigated with or without the presence of 10 μM ICG-001 (Selleck Chemicals LLC, Houston, TX, USA), a commercial Wnt/β-catenin inhibitor. On day 7 of cultivation, cells were collected and performed to RT-qPCR and western blotting analysis using the same methods as described in Section 2.5. On day 14 of cultivation, a BCIP/NBT alkaline phosphatase (ALP) color development kit (Beyotime, China) was used to perform alkaline phosphatase staining for cells in different groups.

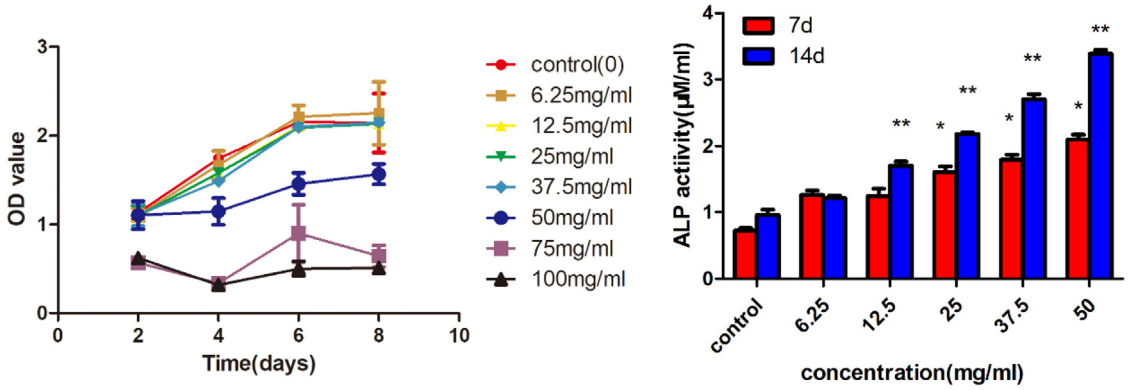

Fig. 1. The effect of different concentration of LCS extracts on the proliferation and the ALP activity of PDLCs. LCS extracts significantly enhanced the ALP activity of PDLCs. *: Significant difference ($p < 0.05$) compared to blank control on day 7. **: Significant difference ($p < 0.05$) compared to blank control on day 14.

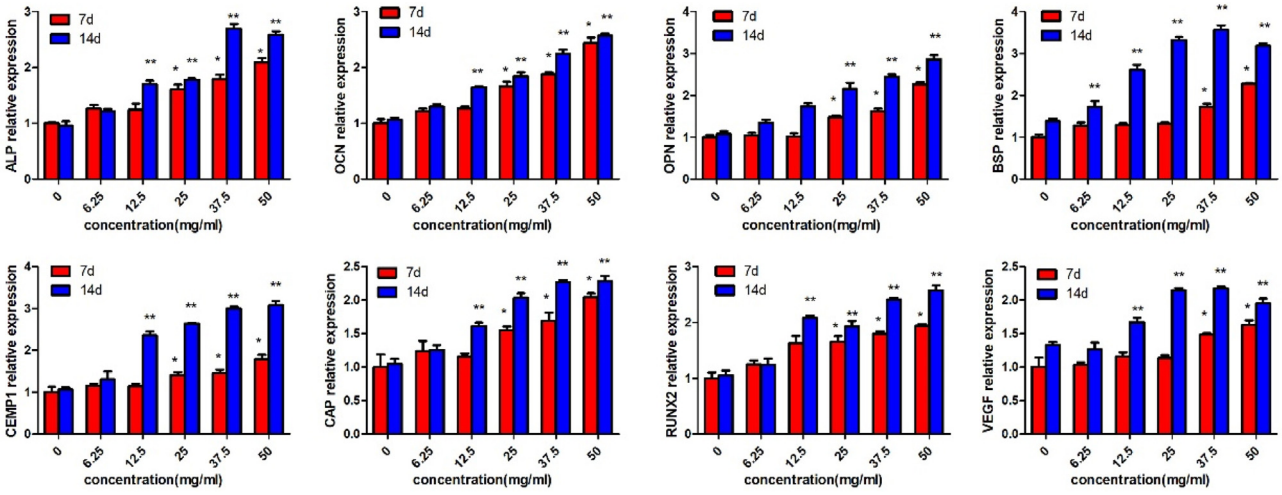

Fig. 2. The effect of LCS extracts on osteogenic/cementogenic gene expression (ALP, OPN, OCN, BSP, CAP, CEMP1, VEGF, RUNX2) of PDLCs by RT-qPCR. LCS extracts could significantly stimulate osteogenic/cementogenic gene expression of PDLCs. *: $p < 0.05$ compared to 0 mg/mL on day 7. **: $p < 0.05$ compared to 0 mg/mL on day 14.

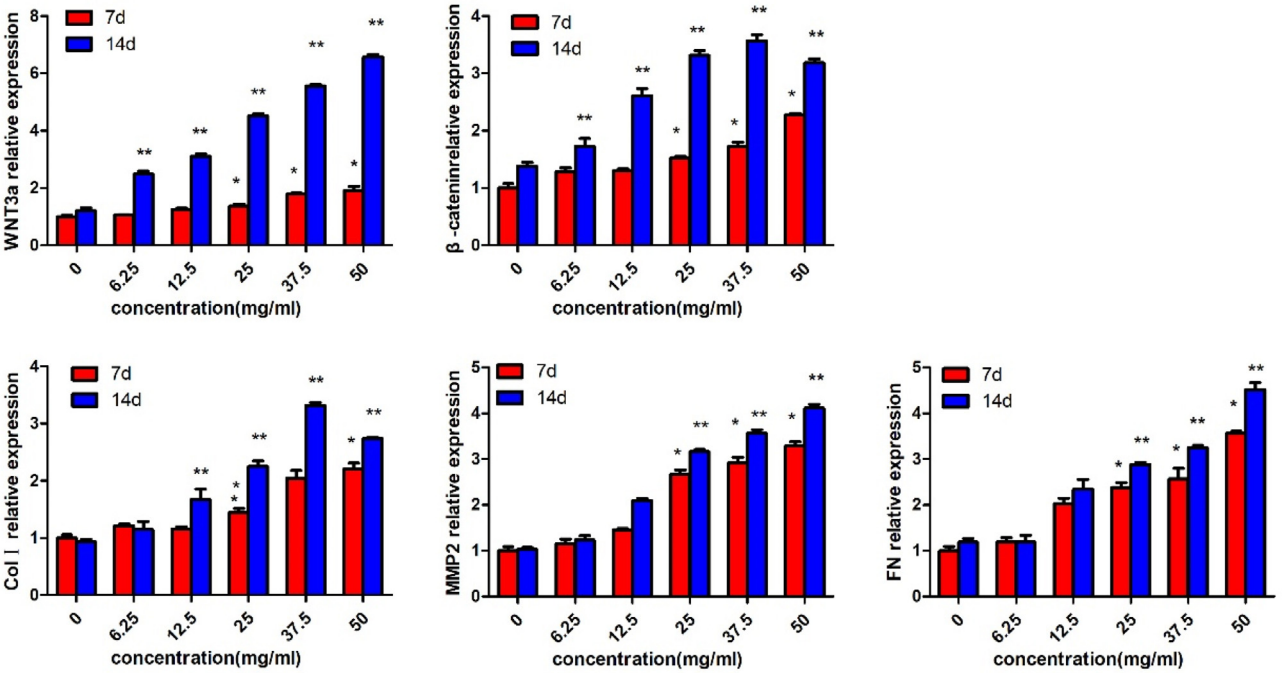

Fig. 3. The effect of LCS extracts on Wnt/β-catenin and ERK signaling pathway related gene expression (wnt3a, β-catenin, p65, MMP2, FN and coll) of PDLCs by RT-qPCR. LCS extracts could significantly stimulate Wnt/β-catenin and ERK signaling pathway related gene expression (wnt3a, β-catenin, MMP2, FN and coll) of PDLCs. *: $p < 0.05$ compared to 0 mg/mL on day 7. **: $p < 0.05$ compared to 0 mg/mL on day 14.

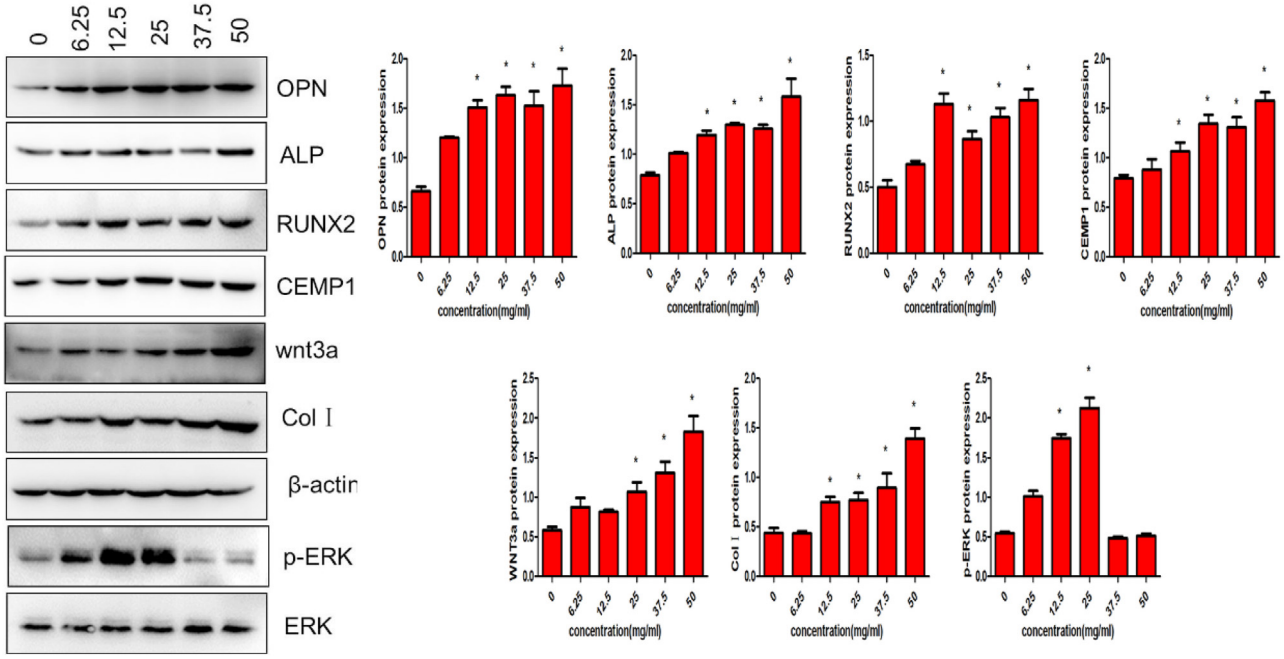

Fig. 4. Western blotting analysis of a series of proteins of PDLCs cultured in the presence of LCS extracts on day 7. The protein expression (ALP, OPN, RUNX2, CEMP1, wnt3a, colI and p-ERK) of PDLCs on were significantly enhanced by the LCS extracts. *: $p < 0.05$ compared to 0 mg/mL.

Similarly, the effect of the ERK signaling pathway on hPDLCs cultured in LCS extracts was investigated with or without the presence of 10 μM SCH772984 (Selleck Chemicals LLC, Houston, TX, USA), a ERK inhibitor, the related genes and proteins are detected.

2.7. *The* in vivo *regeneration of alveolar bone defects for LCS in rabbit models*

A total of 12 male New Zealand white rabbits weighing between 2.5 kg and 3 kg were provided by Nanjing University's Model Animal Research Center. The animal experimental ethics was approved by Nanjing University Ethic Committee. Total 24 mandible defects in 12 rabbits were randomly divided into 3 groups: blank control group, β-TCP group, and LCS group, with 8 samples in each group. Approximately 15 mm incision was made along the upper edge skin of the rabbit mandible under general anesthesia, the lower muscular layer was bluntly separated and the distal of rabbit mandibular incisor was exposed. The alveolar bone on the edentulous region was fully exposed, and the periosteum was separated. A manual electric drill and a ball drill with a 1.5-mm diameter tip were used to make a defect of about 10 mm × 4 mm × 3 mm on the upper edge of the exposed mandible. The trailing edge of the defect was located 2 mm in front of the mental foramen, and the lower edge was flush with the mental foramen. The LCS and β-TCP granules with the size of 420–840 μm were placed respectively into the prepared alveolar defect in groups. No material was placed in the blank control group. Then the incision was closed and sewn in layers. Rabbits were treated with penicillin for 3 days. Four and eight weeks after surgery, all rabbits were euthanized by overdose with anesthetics in two batches respectively.

The mandibles were completely dissected from each rabbit and fixed in 4% paraformaldehyde for 48 h and then flushed overnight with water. The mandible was decalcified by 10% EDTA solution for 3 months. The decalcifying fluid was changed every 3 days. After decalcification, the specimen were dehydrated with a gradient series of ethanol and embedded in paraffin. The specimen was then sectioned and observed under a microscope. Histological sections were cut into 4 μm-thick sections and stained by using HE and MASSON methods. Moreover, immunohistochemical staining on BMP2 and VEGF were made in different groups in mandible of periodontal defects in rabbits at 4 weeks. Tissue regeneration was observed under a microscope and photographed.

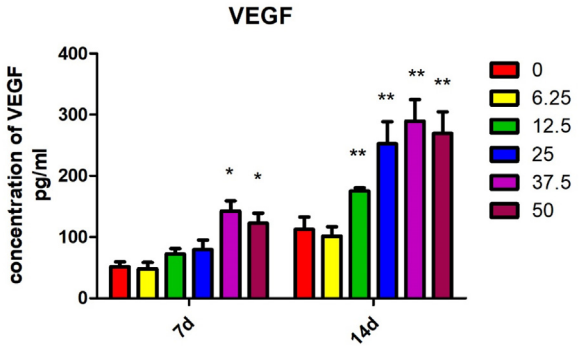

Fig. 5. Concentration of VEGF in PDLCs supernatants at 7 days and 14 days after cultured in the presence of LCS extracts. VEGF concentrations in the supernatant of the PDLCs in LCS extracts were significantly higher than in the blank control groups. *: $p < 0.05$ compared to 0 mg/mL on day 7. **: $p < 0.05$ compared to 0 mg/mL on day 14.

2.8. *The* in vivo *periodontal regeneration of root furcation defects for LCS in beagle dog models*

Four male beagle dogs, one year of age and weighing between 12 and 15 kg, were used in this study. The animal experimental protocol was approved by Nanjing University Ethic Committee. 24 class II root furcation defects were randomly assigned to 3 treatment groups: LCS groups, β-TCP groups and blank control groups. Each group has 8 samples.

The surgical procedures were performed under general anesthesia. Triangle-shaped defects of 5 mm apico-coronally, 4 mm mesiodistally and 3 mm buccolingually were surgically created in the mandibular second, third and fourth premolars by dental turbine. The root periodontal membrane was removed with Gracey

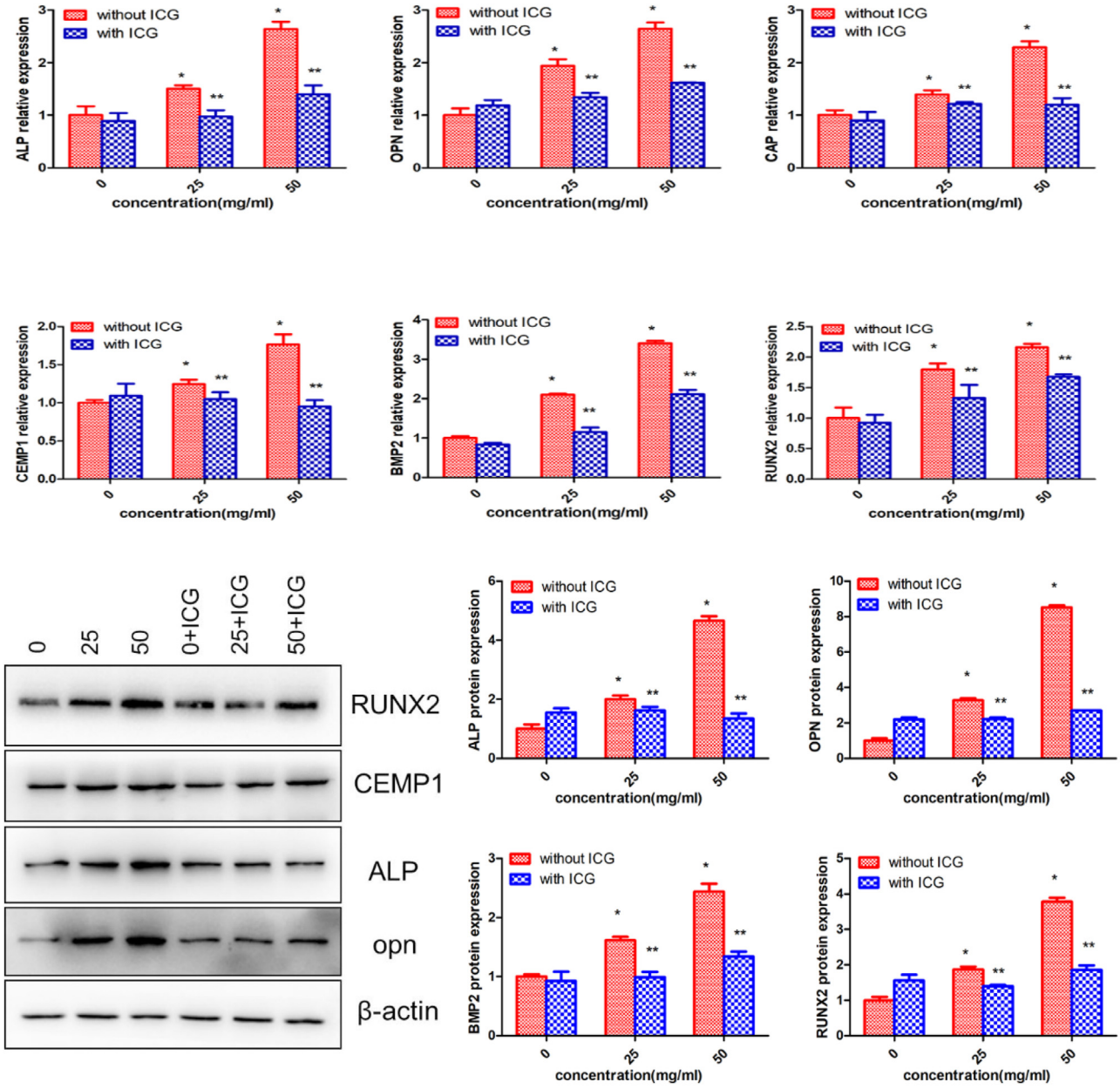

Fig. 6. The effect of blockade of the Wnt/β-catenin signaling pathway on the cementogenic/osteogenic differentiation of PDLCs cultured in the presence of LCS bioceramic extracts (0, 25 and 50 mg/mL) with 10 μM ICG on day 7. The Wnt/β-catenin signaling pathway inhibitor had a significant inhibitory effect on the osteogenic/cementogenic differentiation of PDLCs. *: $p < 0.05$ compared to 0 mg/mL without ICG. **: $p < 0.05$ compared to the same concentration with supplementation of ICG.

curettes. Heat-softened gutta-percha was placed into the defect area, and the wound was sutured. The small dose of antibiotics was administered for three days. 6 weeks after the defects were prepared, an experimental model of chronic II° bifurcation lesions can be formed.

Then the full-thickness flap was made to remove the granulation tissue, cementum and gutta-percha using curettes. The LCS and β-TCP granules were placed respectively into the prepared periodontal defect in groups, no material was placed as the blank control groups. Then 6 mm × 5 mm Bio-Gide membranes were placed onto the periodontal defect surface as a barrier membrane. The incision was closed and sewn in layers.

12 weeks after the placement surgery, the dogs were euthanized by overdose with anesthetics to harvest the specimens. Cone beam CT (CBCT) was used to observe the osteogenesis of the root bifurcation defect, and the difference in osteogenic ability between the groups was compared. The CBCT imaging system (newtom CBCT, Italy) was used to perform the tomographic data scanning and 3D reconstruction of the acquired mandibular tissue specimens. The acquired images were combined with the relevant measurement software for the following analysis. Subsequently, the specimens were fixed in 10% buffered formalin and embedded in paraffin for morphological analysis. Histological sections were cut into 4 μm-thick sections and stained by using HE and MASSON methods.

2.9. Statistical analysis

The data were analyzed by the statistical software SPSS 20.0 (Chinese version). Graphs were generated in GraphPad Prism version 5 for Windows (GraphPad Software, USA). The experimental data for each group is expressed as mean ± standard deviation (SD). One-way ANOVA with a post hoc test was used to analyze these

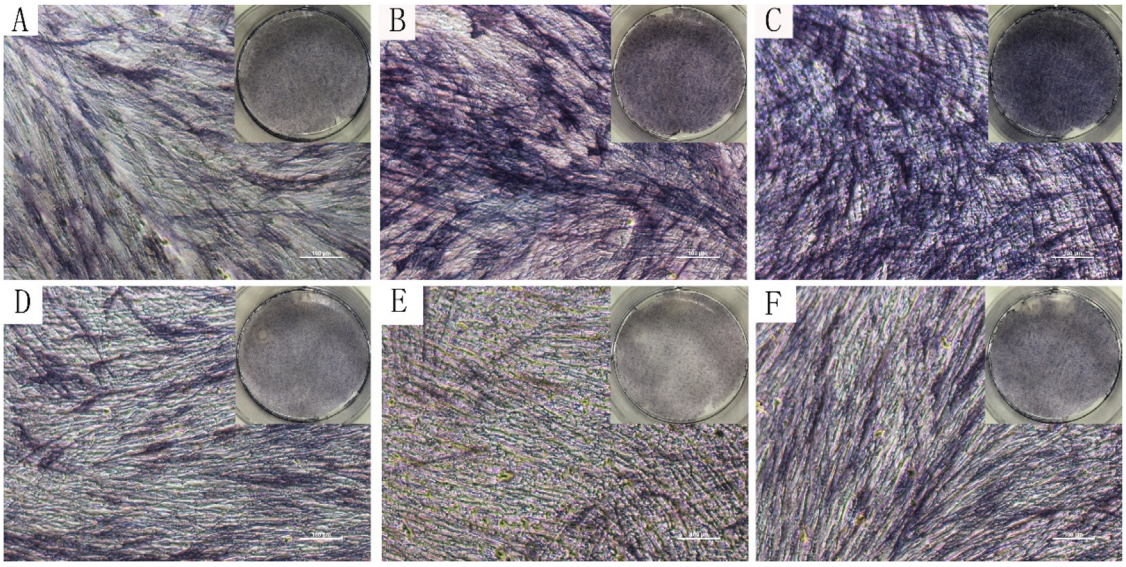

Fig. 7. Alkaline phosphatase staining showing that blockade of the Wnt/β-catenin signaling pathway had a negative effect on the ALP deposition of PDLCs. (A) 0 mg/mL of LCS; (B) 25 mg/mL of LCS; (C) 50 mg/mL of LCS; (D) A with 10 μM ICG; (E) B with 10 μM ICG; (F) C with 10 μM ICG.

data. Statistical significance was considered at the probability level $p < 0.05$.

3. Results

3.1. The effect of LCS extracts on the proliferation activity and alkaline phosphatase (ALP) activity of hPDLCs

CCk-8 results showed that a certain concentration of LCS did not affect the proliferation of PDLCs as shown in Fig. 1, the difference was not statistically significant compared to the blank control group, but high concentrations of LCS resulted in the death of PDLCs. At a concentration of 50 mg/mL of LCS, the proliferation of cells slowed down. Thus, the highest concentration of LCS extracts in the subsequent experiments was set to 50 mg/mL.

Compared with the blank control group, the ALP activity of the PDLCs was significantly enhanced after 7 days of culture at a certain concentration (25, 37.5, 50 mg/mL) of LCS (Fig. 1), and the difference was statistically significant ($p < 0.05$). After 14 days of culture at a certain concentration (12.5, 25, 37.5, 50 mg/mL) of LCS extracts, the ALP activity of PDLCs significantly increased (Fig. 1), and the effect is concentration dependent and time dependent.

3.2. The effect of LCS extracts on osteogenic/cementogenic differentiation and angiogenic gene/protein expression of hPDLCs

Results of real-time PCR showed that, as shown in Fig. 2, a certain concentration of LCS extracts can significantly promote osteogenic/cementogenic differentiation of PDLCs to different degrees on both day 7 and 14, compared with the blank control group. The stimulatory effect depended on the concentrations of LCS, in which the highest values of the gene expression of ALP, OPN, OCN, BSP, CAP, CEMP1, VEGF, Runx2 were shown at 50 mg/mL. In addition, the LCS extracts can significantly enhance the expression of the Wnt/β-catenin pathway-related genes (wnt3a, β-catenin) and the ERK pathway-related genes (MMP2, FN and col I) in the PDLCs on both day 7 and 14, as shown in Fig. 3, compared with the blank control group. The stimulatory effect has a certain concentration dependence, and the promotion of LCS at 50 mg/mL is most distinct.

The protein expression results were almost consistent with the gene expression profiles, as shown in Fig. 4. The promotion of LCS at 50 mg/mL was most pronounced. These results suggest that LCS may activate the Wnt/β-catenin and the ERK signaling pathways to promote osteogenic/cementogenic and angiogenic differentiation of PDLCs.

After cultivation in LCS extracts for 7 days, VEGF concentrations in the supernatant of the PDLCs were significantly higher than in the blank control groups. The concentration of VEGF of PDLCs depended on the concentration of LCS extracts, in which the highest value was shown in **37.5 mg/mL** extracts (Fig. 5, $p < 0.05$). A similar trend of the VEGF concentrations in PDLCs cultured in the extracts for 14 days was also observed, as shown in Fig. 5 ($p < 0.05$).

3.3. The effects of Wnt/β-catenin and ERK signaling pathways on osteogenic/cementogenic differentiation of hPDLCs cultured in LCS extracts

RT-qPCR results (Fig. 6) showed that Wnt/β-catenin signaling pathway inhibitor ICG-001 had a significant inhibitory effect on the expression of the osteogenic/cementogenic genes (ALP, OPN, CAP, CEMP1, BMP-2, and Runx2) in PDLCs cultured with LCS extracts. However, the ICG-001 could not completely counteract the promotion of expression of cementogenic/osteogenic genes of PDLCs cultured in LCS extracts as compared to that of the control group, as seen in Fig. 6. Western blotting analysis further confirmed the effects (Fig. 6).

Alkaline phosphatase (ALP) staining results showed that 25 and 50 mg/mL LCS extracts could significantly enhance the deposition of ALP in PDLCs, and this effect was significantly inhibited after the addition of Wnt/β-catenin signaling pathway inhibitor ICG-001, as shown in Fig. 7.

Similarly, ERK signaling pathway inhibitor SCH772984 had a significant inhibitory effect on the expression of the genes (Runx2, MMP2, FN, Col I, PDGF, and EGF) and the proteins (p-p65, MMP2, p-ERK) in PDLCs cultured in LCS extracts, compared to at the same LCS concentration without SCH772984 (Fig. 8).

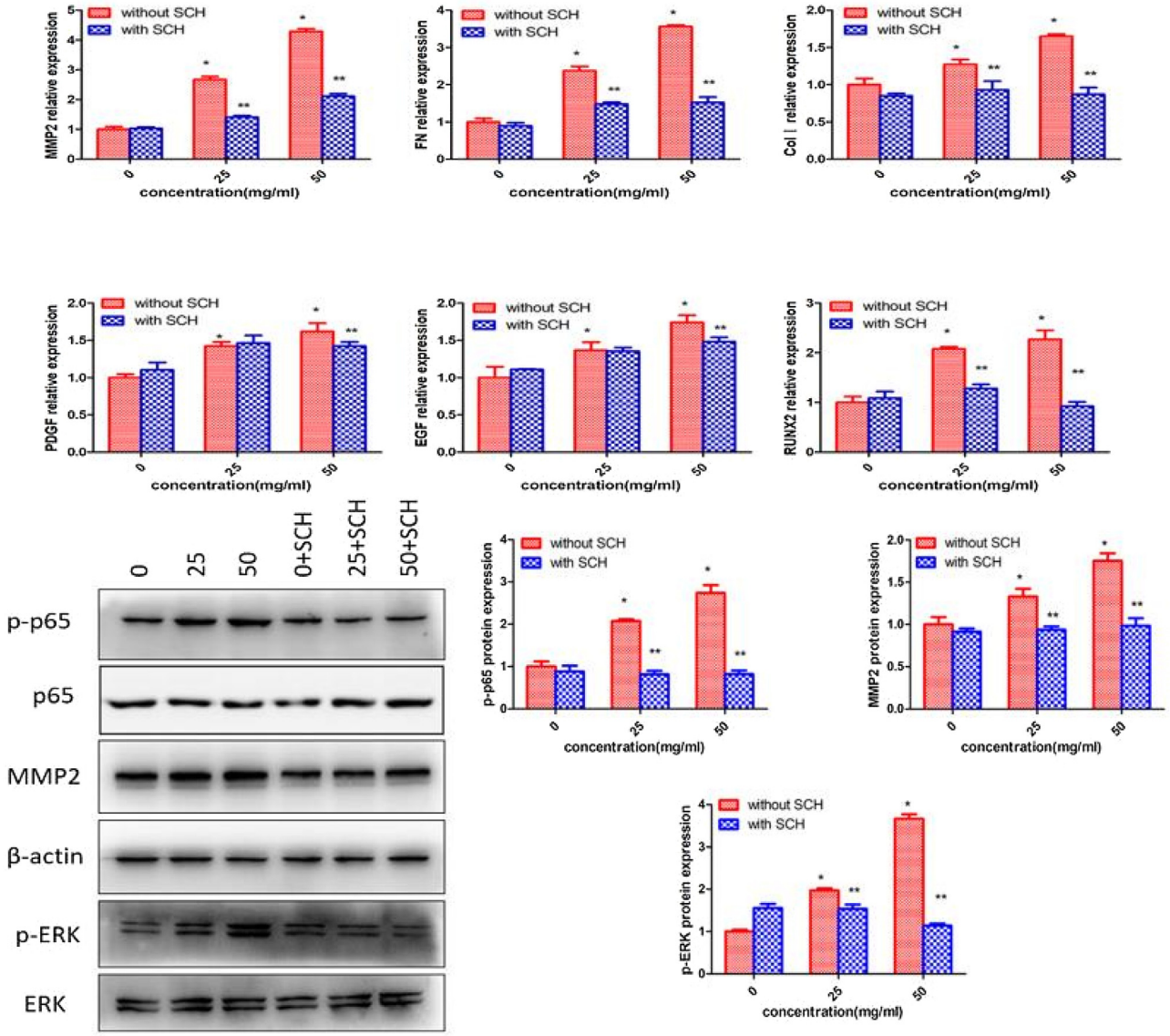

Fig. 8. The effect of blockade of the ERK signaling pathway on the cementogenic/osteogenic differentiation of PDLCs cultured in the presence of LCS bioceramic extracts (0, 25 and 50 mg/mL) with 10 μM SCH on day 7. The ERK signaling pathway inhibitor had a significant inhibitory effect on the osteogenic/cementogenic differentiation. *: $p < 0.05$ compared to 0 mg/mL without SCH; **: $p < 0.05$ compared to the same concentration with supplementation of SCH.

3.4. *The* in vivo *regeneration of alveolar bone defects for LCS in rabbit models*

After implanted for 4 weeks, the specimens were stained with HE, as shown in Fig. 9, histological observation showed that the regeneration of alveolar bone in different degrees were observed in three groups. There were more new bone formation on the LCS groups than the other groups and osteoblasts were more common and osteogenic activity was active. However, there were some undegraded materials could be found in LCS and β-TCP groups. Immunohistochemical staining of the repair of alveolar defects in three groups at 4 weeks showed more VEGF and BMP2 (osteogenic and angiogenic markers) positive markers in LCS groups compared to the others (Fig. 10).

At 8 weeks after surgery (Fig. 9), there were more new bone formations and osteoblasts on the LCS groups, and the trabecular of bones were more mature in the morphology and structure than that two groups. In Masson staining, the newly developed alveolar bone had a higher maturity were stained in red and low maturity in blue. As shown in Fig. 9, the newly bone were more mature in LCS groups.

3.5. *The* in vivo *periodontal regeneration of root furcation defects for LCS in beagle dog models*

50 of consecutive sections of the experimental tooth were selected as the CBCT measurement area, and the bone repair of the measurement area were quantitatively analyzed, the CBCT images were shown in Supplementary Fig. 1. The results showed that the bone mineral density and the volume of the measured bifurcation area were significantly higher in LCS groups than those in the β-TCP groups and the blank control after implanted for 12 weeks (Fig. 11).

Similarly, the HE staining showed the blank control groups, β-TCP groups had obvious inflammatory cell infiltration, and the newborn alveolar bone and cementum were less. However, the LCS groups had a large number of connective tissue ingrowth, filling most of the area of the root bifurcation, with more amount of new bone and cementum. Moreover, there were more mature

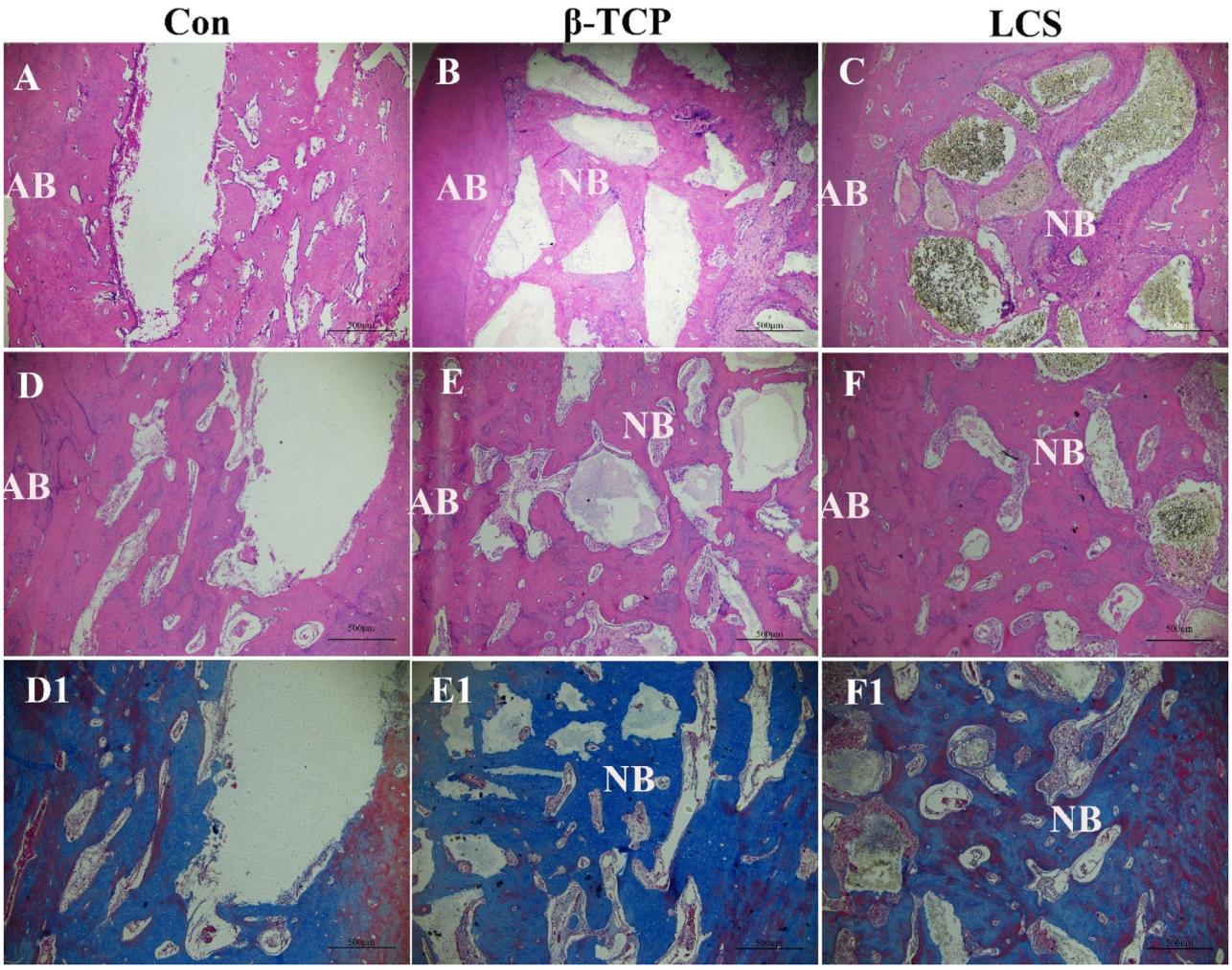

Fig. 9. The regeneration quality of alveolar bone in mandible of periodontal defects in rabbits at 4 and 8 weeks of post-surgery. (A–F) H&E staining at 4 weeks (A–C) and 8 weeks (D–F) of post-surgery. D1–F1: Masson staining at 8 weeks of post-surgery, the newly developed alveolar bone had a higher maturity were stained in red and low maturity in blue. NB: newly bone; AB: alveolar bone. A, D and D1: control groups; B, E and E1: β-TCP groups; C, F, F1: LCS groups. It demonstrated that LCS groups possessed considerable amount of alveolar bone regeneration as compared to the other two experimental groups at week 8. Scale bar: 500 μm. (For interpretation of the references to color in this figure legend, the reader is referred to the web version of the article.)

newborn bone in LCS groups which stained in red compared with blank control groups, β-TCP groups (Fig. 11).

4. Discussion

Periodontitis is a common chronic oral disease, with a high incidence in the human population, which can cause damage to the alveolar bone, loss of periodontal attachment, and eventually loss of teeth [29,30]. It is difficult to regenerate damaged periodontal tissues including gingiva, periodontal ligament, alveolar bone and cementum. Thus, it is of great challenging to treat the chronic periodontitis. Traditional periodontal treatment, including the clinically widely used periodontal guided tissue regeneration (GTR), can significantly improve the repair of periodontal tissue defects [31–33], but still cannot help the damaged periodontal tissue to be fully regenerated. Synthetic biomaterials are used for periodontal regenerative applications. They have no risk for cross infection/disease transmission, which make it possible for periodontal regeneration. In order to achieve the ultimate goal of periodontal tissue engineering, bioactive materials should promote the osteogenic/cementogenic/angiogenic differentiation of PDLCs and stimulate the regeneration of periodontal tissues. Unfortunately, the current biomaterials have not been found to possess the ability for stimulating osteogenic/cementogenic/angiogenic differentiation of PDLCs and for fully periodontal regeneration despite a great number of studies have been conducted.

Silicate bioceramics have been widely used for bone tissue regeneration for their good characteristics in bone formation, many recent studies have achieved better bone regeneration results [34–37]. Meanwhile, because of the application of Li in the repair of bone-cartilage and the role of Li in promoting the differentiation of periodontal ligament cells *in vitro*, we consider the synergistic effect of these ions could promote periodontal regeneration.

One of major novelty of this study is that we found that Li, Si, Ca-containing ionic products from LCS extracts could significantly stimulated the proliferation and osteogenic/cementogenic/angiogenic differentiation of PDLCs, which were crucial process in the regeneration of periodontal tissues. It is speculated that Li, Si and Ca ions may have synergistic role in enhancing the periodontal regeneration. Wnt signaling plays a central role in many processes during embryonic development and human homeostasis. The Wnt/β-catenin signaling pathway plays an important role in bone reconstruction and tooth

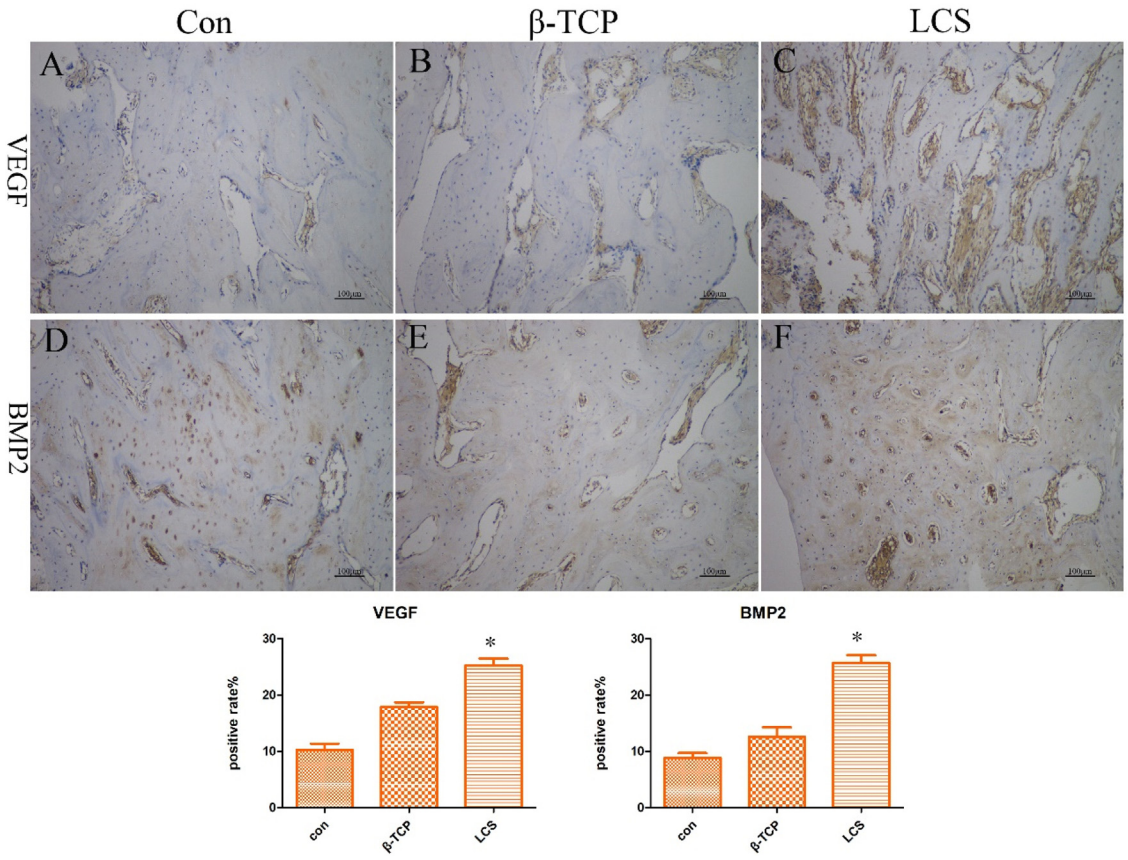

Fig. 10. Immunohistochemical staining of the repair of periodontal defects in different groups in mandible of periodontal defects of rabbits at 4 weeks. More VEGF and BMP2 (osteogenic and angiogenic markers) positive markers in LCS groups were found than the others. Scale bar: 100 μm. *, compared with control and β-TCP groups, $p < 0.05$.

regeneration [38–40]. It was found that the Wnt/β-catenin signaling pathway promotes osteogenic differentiation of periodontal ligament fibroblasts and cementum regeneration [41,42]. After activation of the Wnt/β-catenin signaling pathway, the Wnt/β-catenin signaling pathway can regulate the balance between the receptor activator of nuclear factor κ-B ligand and osteoprotegerin and enhance the osteogenic differentiation [43]. Some researchers believed that silicate-based bioceramics promoted proliferation and osteogenic differentiation of bone marrow stromal stem cells because they activated Wnt signaling pathway [28,44]. Similarly, Li could activate Wnt/β-catenin signaling pathway by inhibiting the degradation of GSK-3β in Wnt/β-catenin, leading to promote cell proliferation and cementogenic and osteogenic differentiation of periodontal ligament cells, bone marrow-derived mesenchymal stem cells and osteoblasts [45–48]. In this study, we investigated whether the role of LCS in promoting periodontal differentiation was due to the activation of the Wnt/β-catenin signaling pathway. The results showed that the Wnt/β-catenin signaling pathway was activated in response to the LCS extracts. Furthermore, after addition with the Wnt/β-catenin inhibitor, ICG-001, led to a decrease in osteogenic gene expression of ALP, OPN, Runx2 and BMP2, together with the reduced expression of cementogenic genes, CAP and CEMP1 as well as the corresponding protein synthesis. In addition, previous studies had shown that the ERK pathway can also promote osteogenic differentiation of PDLCs [49–52], and can also promote the differentiation of PDLCs into neural Schwann cells [53]. Other studies had shown that a natural active substance extracted from black tea can inhibit osteoclastogenesis and inhibit osteoclast bone resorption by inhibiting RANKL-induced ERK pathway [54]. Similarly, in the present study, the ERK signaling pathway was investigated, and our results showed that the LCS could up-regulate the expression of ERK pathway-related genes and proteins, and down-regulate their expression after using ERK pathway inhibitors. Therefore, it is reasonable to speculate that the mechanism for LCS promoting osteogenic/cementogenic/angiogenic differentiation of PDLCs is closely related to the activation of Wnt/β-catenin and ERK signaling pathways by releasing of Li and Si ions from LCS bioceramics.

The other important novelty of the study is that we found LCS have shown significantly stimulatory effect on periodontal regeneration both in rabbit and beagle dog models. To our knowledge, although the use of bioactive ions as a reagent for promoting bone formation has been well studied, the role of the released ions from bioceramics in the periodontitis models is not fully investigated. In our study, according to our previous methods [55], acute root bifurcation defects were established, and the gutta-percha were placed. After 6 weeks, the chronic periodontal inflammation was formed, indicating that chronic II° bifurcation lesion models were successfully constructed. This modeling method could well simulate the development of human periodontitis.

Then LCS granules were used to implant in the rabbit mandible and beagle dog models. The histological results in rabbits showed there were more new bone in LCS groups, and more BMP2 and VEGF proteins positive expression were observed in LCS groups, which proved the osteogenesis and angiogenic ability of LCS bioceramics. The quantitative CBCT measurement results in beagle dog models showed higher bone mineral density and bone volume in defect area for LCS than β-TCP groups. The histological results showed the LCS groups had more new alveolar bone, new periodontal ligament and new cementum-like tissue growth than the β-TCP groups. In the LCS groups, the new alveolar bone, the mineralization of which

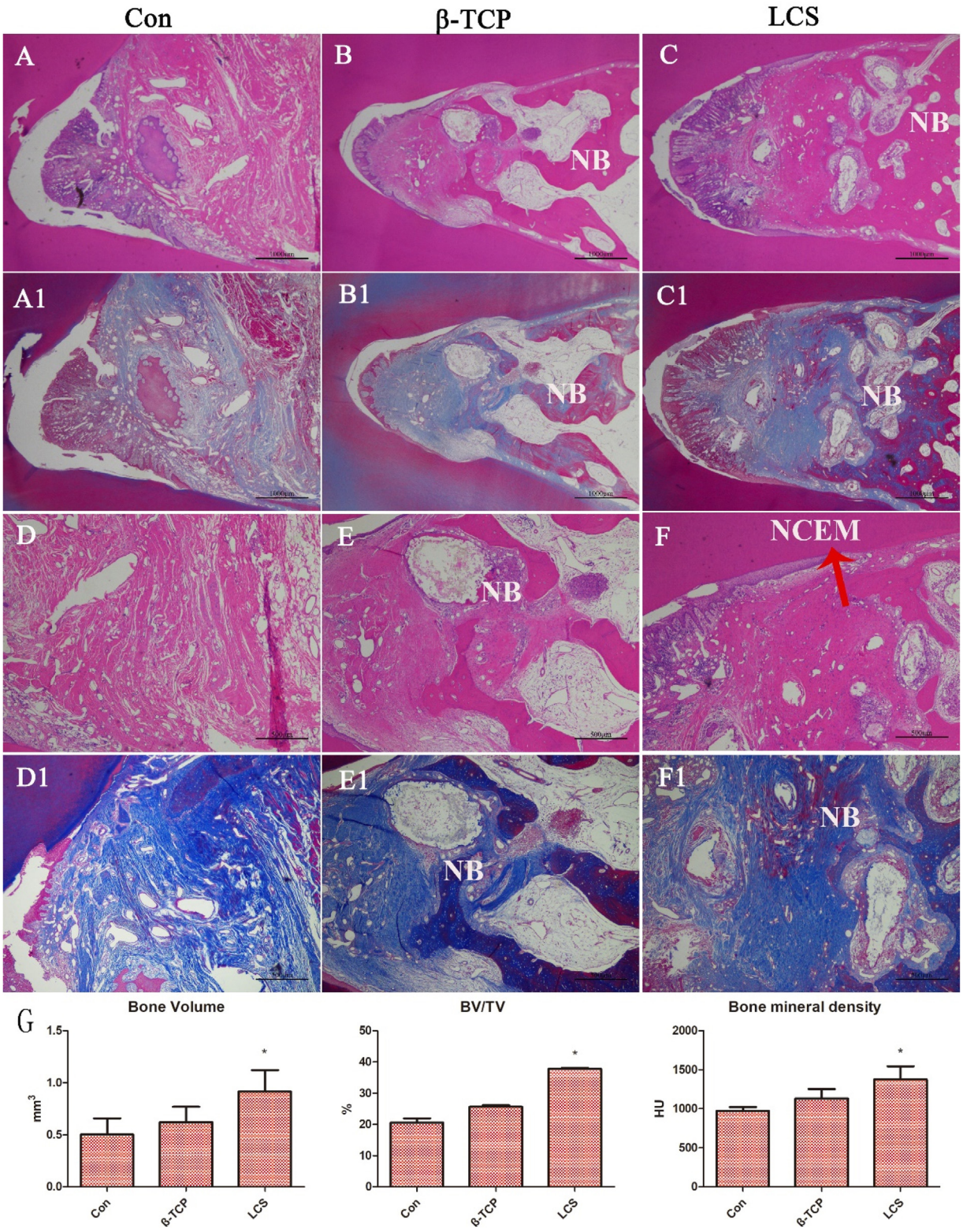

Fig. 11. Periodontal regeneration of the root bifurcation in beagle dogs of each group at 12 weeks after regeneration. (A–F) H&E staining at 12 weeks of post-surgery. (A1–F1) Masson staining at 12 weeks of post-surgery. (G) Bone mass at root bifurcation in beagle dogs in three groups in 12 weeks after regeneration. BV, bone volume; TV, tissue volume; BMD, bone mineral density. (A–C, A1–C1) Scale bar: 100 μm. (D–F, D1–F1) Scale bar: 500 μm. The bone mineral density and the volume of the measured bifurcation area were significantly higher in LCS groups than those in the β-TCP groups and the blank control, and there were more mature newborn bone in LCS groups which stained in red compared with blank control groups, β-TCP groups. NB: newly bone; AB: alveolar bone; NCEM: newly formed cementum-like tissue. *, compared with control and β-TCP groups, $p < 0.05$. (For interpretation of the references to color in this figure legend, the reader is referred to the web version of the article.)

was low, was observed from the root to the crown, and integrated with the original alveolar bone. The newly formed cementum-like tissue was discontinuously covered the bare root surface. Neonatal periodontal ligament was observed between the new cementum and the new alveolar bone.

Current studies indicate that the Wnt/β-catenin pathway is associated with periodontal ligament cells with their surrounding inflammatory micro-environment [56,57]. PDLSCs under inflammatory conditions could result in the reduction in the osteogenic differentiation capacity and mineralized nodule formation [56]. Canonical Wnt/β-catenin pathway could regulate the osteogenic differentiation potential of PDLCs in the presence of inflammation [58]. Our previous study demonstrated that the osteogenic differentiation of PDLCs was significantly promoted in inflammatory microenvironments via activating the Wnt/β-catenin signaling pathway [59]. In addition, studies have shown that LiCl can treat bone destruction caused by periapical lesions by activating the Wnt/β-catenin signaling [60]. Therefore, we speculate that LCS may be a potential therapeutic option for periodontal bone destruction in periodontal disease. In our present study, the periodontitis defect models were shown that LCS granules play a better role in periodontal regeneration than conventional β-TCP, indicating that the LCS can effectively promote the regeneration of periodontal tissues under inflammatory microenvironment. Based on the results of cell culture, it is reasonable to speculate that the role of LCS in periodontal regeneration may be related to its stimulatory effect on the osteogenic/cementogenic/angiogenic differentiation of PDLCs via activating the Wnt/ERK signaling pathways.

Thus, in the study, we, for the first time, combined the medium and large animal models to explore the regeneration activity of LCS bioceramcis, further proving its significance for periodontal regeneration. The *in vivo* studies demonstrates that even in the case of LCS alone, it can effectively promote periodontal regeneration, indicating that LCS is a promising biomaterial for periodontal regeneration.

5. Conclusion

The present study showed that the LCS bioceramics significantly enhanced the ALP activity, osteogenic/cementogenic and angiogenic differentiation of PDLCs by combining the synergistic effects of Li, Ca and Si ions. The significantly stimulatory effects of LCS bioceramics on PDLCs differentiation toward to osteogenesis, cementogenesis and angiogenesis are closely related to the activation of Wnt/β-catenin and ERK signaling pathways of PDLCs. The LCS bioceramics possess the capacity to distinctly enhance the periodontal regeneration both in rabbit and beagle dog models. Our results indicate that LCS bioceramics may be used for periodontal regeneration, offering a new treatment strategy for the treatment of periodontitis.

Data availability

The authors declare that all data supporting the findings of this study are available within the paper.

Conflict of interests

The authors state that there are no conflicts of interest associated with this study and the publication of this manuscript.

Acknowledgements

This work was supported by the National Key Research and Development Program of China (2018YFC1105201), the National Natural Science Foundation of China (81570982, 5171101275), Innovation Cross Team of Chinese Academy Sciences (JCTD-2018-13) and Science and Technology Commission of Shanghai Municipality (17540712300).

Appendix A. Supplementary data

Supplementary data associated with this article can be found, in the online version, at doi:10.1016/j.apmt.2019.06.011.

References

[1] M. Bansal, S. Rastogi, N.S. Vineeth, Influence of periodontal disease on systemic disease: inversion of a paradigm: a review, J. Med. Life 6 (2) (2013) 126–130.
[2] M. Sanz, A. Ceriello, M. Buysschaert, I. Chapple, R.T. Demmer, F. Graziani, D. Herrera, S. Jepsen, L. Lione, P. Madianos, M. Mathur, E. Montanya, L. Shapira, M. Tonetti, D. Vegh, Scientific evidence on the links between periodontal diseases and diabetes: consensus report and guidelines of the joint workshop on periodontal diseases and diabetes by the International Diabetes Federation and the European Federation of Periodontology, J. Clin. Periodontol. 45 (2) (2018) 138–149.
[3] A. Sculean, D. Nikolidakis, G. Nikou, A. Ivanovic, I.L. Chapple, A. Stavropoulos, Biomaterials for promoting periodontal regeneration in human intrabony defects: a systematic review, Periodontol. 2000 68 (1) (2015) 182–216.
[4] R.T. Kao, S. Nares, M.A. Reynolds, Periodontal regeneration – intrabony defects: a systematic review from the AAP Regeneration Workshop, J. Periodontol. 86 (2 Suppl.) (2015) S77–S104.
[5] Z. Sheikh, N. Hamdan, Y. Ikeda, M. Grynpas, B. Ganss, M. Glogauer, Natural graft tissues and synthetic biomaterials for periodontal and alveolar bone reconstructive applications: a review, Biomater. Res. 21 (2017) 9.
[6] X. Liu, Q. Li, F. Wang, Z. Wang, Maxillary sinus floor augmentation and dental implant placement using dentin matrix protein-1 gene-modified bone marrow stromal cells mixed with deproteinized boving bone: a comparative study in beagles, Arch. Oral Biol. 64 (2016) 102–108.
[7] M. Yildirim, H. Spiekermann, S. Biesterfeld, D. Edelhoff, Maxillary sinus augmentation using xenogenic bone substitute material Bio-Oss in combination with venous blood. A histologic and histomorphometric study in humans, Clin. Oral Implants Res. 11 (3) (2000) 217–229.
[8] P. Felice, C. Marchetti, G. Iezzi, A. Piattelli, H. Worthington, G. Pellegrino, M. Esposito, Vertical ridge augmentation of the atrophic posterior mandible with interpositional bloc grafts: bone from the iliac crest vs. bovine anorganic bone. Clinical and histological results up to one year after loading from a randomized-controlled clinical trial, Clin. Oral Implants Res. 20 (12) (2009) 1386–1393.
[9] H.C. Aludden, A. Mordenfeld, M. Hallman, C. Dahlin, T. Jensen, Lateral ridge augmentation with Bio-Oss alone or Bio-Oss mixed with particulate autogenous bone graft: a systematic review, Int. J. Oral Maxillofac. Surg. 46 (8) (2017) 1030–1038.
[10] C. Wu, J. Chang, A review of bioactive silicate ceramics, Biomed. Mater. 8 (3) (2013) 032001.
[11] I.D. Ana, G.A.P. Satria, A.H. Dewi, R. Ardhani, Bioceramics for clinical application in regenerative dentistry, Adv. Exp. Med. Biol. 1077 (2018) 309–316.
[12] W. Zhang, C. Feng, G. Yang, G. Li, X. Ding, S. Wang, Y. Dou, Z. Zhang, J. Chang, C. Wu, X. Jiang, 3D-printed scaffolds with synergistic effect of hollow-pipe structure and bioactive ions for vascularized bone regeneration, Biomaterials 135 (2017) 85–95.
[13] M. Shi, Y. Zhou, J. Shao, Z. Chen, B. Song, J. Chang, C. Wu, Y. Xiao, Stimulation of osteogenesis and angiogenesis of hBMSCs by delivering Si ions and functional drug from mesoporous silica nanospheres, Acta Biomater. 21 (2015) 178–189.
[14] L. Mao, L. Xia, J. Chang, J. Liu, L. Jiang, C. Wu, B. Fang, The synergistic effects of Sr and Si bioactive ions on osteogenesis, osteoclastogenesis and angiogenesis for osteoporotic bone regeneration, Acta Biomater. 61 (2017) 217–232.
[15] C. Wu, Y. Ramaswamy, H. Zreiqat, Porous diopside (CaMgSi(2)O(6)) scaffold: a promising bioactive material for bone tissue engineering, Acta Biomater. 6 (6) (2010) 2237–2245.
[16] C. Wu, Z. Chen, Q. Wu, D. Yi, T. Friis, X. Zheng, J. Chang, X. Jiang, Y. Xiao, Clinoenstatite coatings have high bonding strength, bioactive ion release, and osteoimmunomodulatory effects that enhance in vivo osseointegration, Biomaterials 71 (2015) 35–47.
[17] C. Deng, H. Zhu, J. Li, C. Feng, Q. Yao, L. Wang, J. Chang, C. Wu, Bioactive scaffolds for regeneration of cartilage and subchondral bone interface, Theranostics 8 (7) (2018) 1940–1955.
[18] V. Bunpetch, X. Zhang, T. Li, J. Lin, E.P. Maswikiti, Y. Wu, D. Cai, J. Li, S. Zhang, C. Wu, H. Ouyang, Silicate-based bioceramic scaffolds for dual-lineage regeneration of osteochondral defect, Biomaterials 192 (2019) 323–333.
[19] C.L. Thompson, A. Wiles, C.A. Poole, M.M. Knight, Lithium chloride modulates chondrocyte primary cilia and inhibits Hedgehog signaling, FASEB J. 30 (2) (2016) 716–726.
[20] W. Hui, G.J. Litherland, M. Jefferson, M.J. Barter, M.S. Elias, T.E. Cawston, A.D. Rowan, D.A. Young, Lithium protects cartilage from cytokine-mediated

degradation by reducing collagen-degrading MMP production via inhibition of the P38 mitogen-activated protein kinase pathway, Rheumatology (Oxford) 49 (11) (2010) 2043–2053.
[21] T. Minashima, Y. Zhang, Y. Lee, T. Kirsch, Lithium protects against cartilage degradation in osteoarthritis, Arthritis Rheumatol. 66 (5) (2014) 1228–1236.
[22] L.A. Haro Durand, G.E. Vargas, R. Vera-Mesones, A. Baldi, M.P. Zago, M.A. Fanovich, A.R. Boccaccini, A. Gorustovich, In vitro human umbilical vein endothelial cells response to ionic dissolution products from lithium-containing 45S5 bioactive glass, Materials (Basel) 10 (7) (2017).
[23] Z. Yu, L. Fan, J. Li, Z. Ge, X. Dang, K. Wang, Lithium chloride attenuates the abnormal osteogenic/adipogenic differentiation of bone marrow-derived mesenchymal stem cells obtained from rats with steroid-related osteonecrosis by activating the beta-catenin pathway, Int. J. Mol. Med. 36 (5) (2015) 1264–1272.
[24] Z. Yu, L. Fan, J. Li, Z. Ge, X. Dang, K. Wang, Lithium prevents rat steroid-related osteonecrosis of the femoral head by beta-catenin activation, Endocrine 52 (2) (2016) 380–390.
[25] L. Chen, C. Deng, J. Li, Q. Yao, J. Chang, L. Wang, C. Wu, 3D printing of a lithium-calcium-silicate crystal bioscaffold with dual bioactivities for osteochondral interface reconstruction, Biomaterials 196 (2019) 138–150.
[26] L. Cao, W. Weng, X. Chen, J. Zhang, Q. Zhou, J. Cui, Y. Zhao, J.W. Shin, J. Su, Promotion of in vivo degradability, vascularization and osteogenesis of calcium sulfate-based bone cements containing nanoporous lithium doping magnesium silicate, Int. J. Nanomed. 12 (2017) 1341–1352.
[27] L. Liu, Y. Liu, C. Feng, J. Chang, R. Fu, T. Wu, F. Yu, X. Wang, L. Xia, C. Wu, B. Fang, Lithium-containing biomaterials stimulate bone marrow stromal cell-derived exosomal miR-130a secretion to promote angiogenesis, Biomaterials 192 (2019) 523–536.
[28] Y. Zhou, C. Wu, X. Zhang, P. Han, Y. Xiao, The ionic products from bredigite bioceramics induced cementogenic differentiation of periodontal ligament cells via activation of the Wnt/β-catenin signalling pathway, J. Mater. Chem. B 1 (27) (2013) 3380.
[29] N.J. Kassebaum, E. Bernabe, M. Dahiya, B. Bhandari, C.J. Murray, W. Marcenes, Global burden of severe periodontitis in 1990–2010: a systematic review and meta-regression, J. Dent. Res. 93 (11) (2014) 1045–1053.
[30] J.E. Frencken, P. Sharma, L. Stenhouse, D. Green, D. Laverty, T. Dietrich, Global epidemiology of dental caries and severe periodontitis – a comprehensive review, J. Clin. Periodontol. 44 (Suppl. 18) (2017) S94–S105.
[31] H.C. Hung, C.W. Douglass, Meta-analysis of the effect of scaling and root planning, surgical treatment and antibiotic therapies on periodontal probing depth and attachment loss, J. Clin. Periodontol. 29 (11) (2002) 975–986.
[32] W.V. Giannobile, Commentary: Treatment of periodontitis: destroyed periodontal tissues can be regenerated under certain conditions, J. Periodontol. 85 (9) (2014) 1151–1154.
[33] L. Kostopoulos, T. Karring, Susceptibility of GTR-regenerated periodontal attachment to ligature-induced periodontitis, J. Clin. Periodontol. 31 (5) (2004) 336–340.
[34] Y. Huang, C. Wu, X. Zhang, J. Chang, K. Dai, Regulation of immune response by bioactive ions released from silicate bioceramics for bone regeneration, Acta Biomater. 66 (2018) 81–92.
[35] S. Fu, W. Liu, S. Liu, S. Zhao, Y. Zhu, 3D printed porous beta-Ca_2SiO_4 scaffolds derived from preceramic resin and their physicochemical and biological properties, Sci. Technol. Adv. Mater. 19 (1) (2018) 495–506.
[36] M. Zhu, J. Zhang, S. Zhao, Y. Zhu, Three-dimensional printing of cerium-incorporated mesoporous calcium-silicate scaffolds for bone repair, J. Mater. Sci. 51 (2) (2016) 836–844.
[37] P. Pei, X. Qi, X. Du, M. Zhu, S. Zhao, Y. Zhu, Three-dimensional printing of tricalcium silicate/mesoporous bioactive glass cement scaffolds for bone regeneration, J. Mater. Chem. B 4 (46) (2016) 7452–7463.
[38] C. Hartmann, Skeletal development – Wnts are in control, Mol. Cells 24 (2) (2007) 177–184.
[39] S. Li, J. Shao, Y. Zhou, T. Friis, J. Yao, B. Shi, Y. Xiao, The impact of Wnt signalling and hypoxia on osteogenic and cementogenic differentiation in human periodontal ligament cells, Mol. Med. Rep. 14 (6) (2016) 4975–4982.
[40] M. Tamura, E. Nemoto, Role of the Wnt signaling molecules in the tooth, Jpn. Dent. Sci. Rev. 52 (4) (2016) 75–83.
[41] J.S. Heo, S.Y. Lee, J.C. Lee, Wnt/beta-catenin signaling enhances osteoblastogenic differentiation from human periodontal ligament fibroblasts, Mol. Cells 30 (5) (2010) 449–454.
[42] P. Han, S. Ivanovski, R. Crawford, Y. Xiao, Activation of the canonical Wnt signaling pathway induces cementum regeneration, J. Bone Miner. Res. 30 (7) (2015) 1160–1174.
[43] X. Hu, Z. Wang, J. Shi, X. Guo, L. Wang, Z. Ping, Y. Tao, H. Yang, J. Zhou, Y. Xu, D. Geng, Lithium chloride inhibits titanium particle-induced osteoclastogenesis by inhibiting the NF-kappaB pathway, Oncotarget 8 (48) (2017) 83949–83961.
[44] P. Han, C. Wu, Y. Xiao, The effect of silicate ions on proliferation, osteogenic differentiation and cell signalling pathways (WNT and SHH) of bone marrow stromal cells, Biomater. Sci. 1 (4) (2013) 379–392.
[45] P. Han, C. Wu, J. Chang, Y. Xiao, The cementogenic differentiation of periodontal ligament cells via the activation of Wnt/beta-catenin signalling pathway by Li+ ions released from bioactive scaffolds, Biomaterials 33 (27) (2012) 6370–6379.
[46] P. Han, M. Xu, J. Chang, N. Chakravorty, C. Wu, Y. Xiao, Lithium release from β-tricalcium phosphate inducing cementogenic and osteogenic differentiation of both hPDLCs and hBMSCs, Biomater. Sci. 2 (9) (2014) 1230.
[47] L. Li, R. Wang, B. Li, W. Liang, H. Pan, X. Cui, J. Tang, B. Li, Lithium doped calcium phosphate cement maintains physical mechanical properties and promotes osteoblast proliferation and differentiation, J. Biomed. Mater. Res. B: Appl. Biomater. 105 (5) (2017) 944–952.
[48] L. Tang, Y. Chen, F. Pei, H. Zhang, Lithium chloride modulates adipogenesis and osteogenesis of human bone marrow-derived mesenchymal stem cells, Cell. Physiol. Biochem. 37 (1) (2015) 143–152.
[49] Y. Yan, W. Zeng, S. Song, F. Zhang, W. He, W. Liang, Z. Niu, Vitamin C induces periodontal ligament progenitor cell differentiation via activation of ERK pathway mediated by PELP1, Protein Cell 4 (8) (2013) 620–627.
[50] M. Zhang, P. Zhang, Y. Liu, L. Lv, X. Zhang, H. Liu, Y. Zhou, RSPO3-LGR4 regulates osteogenic differentiation of human adipose-derived stem cells via ERK/FGF signalling, Sci. Rep. 7 (2017) 42841.
[51] M. Tang, Z. Peng, Z. Mai, L. Chen, Q. Mao, Z. Chen, Q. Chen, L. Liu, Y. Wang, H. Ai, Fluid shear stress stimulates osteogenic differentiation of human periodontal ligament cells via the extracellular signal-regulated kinase 1/2 and p38 mitogen-activated protein kinase signaling pathways, J. Periodontol. 85 (12) (2014) 1806–1813.
[52] Y. Wu, Y. Yang, P. Yang, Y. Gu, Z. Zhao, L. Tan, L. Zhao, T. Tang, Y. Li, The osteogenic differentiation of PDLSCs is mediated through MEK/ERK and p38 MAPK signalling under hypoxia, Arch. Oral Biol. 58 (10) (2013) 1357–1368.
[53] L. Dapeng, L. Xiaojie, G. Ping, D. Yan, S. Gang, Erk1/2 signalling is involved in the differentiation of periodontal ligament stem cells to Schwann cells in dog, Arch. Oral Biol. 59 (5) (2014) 487–491.
[54] X. Hu, Z. Ping, M. Gan, Y. Tao, L. Wang, J. Shi, X. Wu, W. Zhang, H. Yang, Y. Xu, Z. Wang, D. Geng, Theaflavin-3,3′-digallate represses osteoclastogenesis and prevents wear debris-induced osteolysis via suppression of ERK pathway, Acta Biomater. 48 (2017) 479–488.
[55] S. Jiang, K. Tang, B. Chen, F. Yan, Regenerative effect of hOPG gene-modified autologous PDLs in combination with cell transplantation on periodontal defection in beagle dogs, Cytotechnology 68 (6) (2016) 2613–2623.
[56] K.M. Fawzy El-Sayed, M. Elahmady, Z. Adawi, N. Aboushadi, A. Elnaggar, M. Eid, N. Hamdy, D. Sanaa, C.E. Dorfer, The periodontal stem/progenitor cell inflammatory-regenerative cross talk: a new perspective, J. Periodontal Res. (2018).
[57] L. Liang, W. Zhou, N. Yang, J. Yu, H. Liu, ET-1 promotes differentiation of periodontal ligament stem cells into osteoblasts through ETR, MAPK, and Wnt/beta-catenin signaling pathways under inflammatory microenvironment, Mediators Inflamm. 2016 (2016) 8467849.
[58] W. Liu, A. Konermann, T. Guo, A. Jager, L. Zhang, Y. Jin, Canonical Wnt signaling differently modulates osteogenic differentiation of mesenchymal stem cells derived from bone marrow and from periodontal ligament under inflammatory conditions, Biochim. Biophys. Acta 1840 (3) (2014) 1125–1134.
[59] J. Zhou, Y. Zhang, L. Li, H. Fu, W. Yang, F. Yan, Human beta-defensin 3-combined gold nanoparticles for enhancement of osteogenic differentiation of human periodontal ligament cells in inflammatory microenvironments, Int. J. Nanomed. 13 (2018) 555–567.
[60] Y. Tang, X. Zhou, B. Gao, X. Xu, J. Sun, L. Cheng, X. Zhou, L. Zheng, Modulation of Wnt/beta-catenin signaling attenuates periapical bone lesions, J. Dent. Res. 93 (2) (2014) 175–182.